Health monitoring of pipeline girth weld using empirical mode decomposition

Smart Mater. Struct. **19** (2010) 055016 (18pp) doi:10.1088/0964-1726/19/5/055016

Health monitoring of pipeline girth weld using empirical mode decomposition

Davood Rezaei and Farid Taheri[1]

Department of Civil and Resource Engineering, Dalhousie University, Halifax, NS, Canada

E-mail: farid.taheri@dal.ca

Received 20 January 2010
Published 31 March 2010
Online at stacks.iop.org/SMS/19/055016

Abstract

In the present paper the Hilbert–Huang transform (HHT), as a time-series analysis technique, has been combined with a local diagnostic approach in an effort to identify flaws in pipeline girth welds. This method is based on monitoring the free vibration signals of the pipe at its healthy and flawed states, and processing the signals through the HHT and its associated signal decomposition technique, known as empirical mode decomposition (EMD). The EMD method decomposes the vibration signals into a collection of intrinsic mode functions (IMFs). The deviations in structural integrity, measured from a healthy-state baseline, are subsequently evaluated by two damage sensitive parameters. The first is a damage index, referred to as the EM-EDI, which is established based on an energy comparison of the first or second IMF of the vibration signals, before and after occurrence of damage. The second parameter is the evaluation of the lag in instantaneous phase, a quantity derived from the HHT. In the developed methodologies, the pipe's free vibration is monitored by piezoceramic sensors and a laser Doppler vibrometer. The effectiveness of the proposed techniques is demonstrated through a set of numerical and experimental studies on a steel pipe with a mid-span girth weld, for both pressurized and nonpressurized conditions. To simulate a crack, a narrow notch is cut on one side of the girth weld. Several damage scenarios, including notches of different depths and at various locations on the pipe, are investigated. Results from both numerical and experimental studies reveal that in all damage cases the sensor located at the notch vicinity could successfully detect the notch and qualitatively predict its severity. The effect of internal pressure on the damage identification method is also monitored. Overall, the results are encouraging and promise the effectiveness of the proposed approaches as inexpensive systems for structural health monitoring purposes.

(Some figures in this article are in colour only in the electronic version)

1. Introduction

The structural health monitoring of pipelines is crucial to insure the safe and reliable flow of energy and to prohibit catastrophic failures. Cracks are a common type of defect that occur in pipelines and weaken the structural integrity of the pipe; and if left undetected, can grow to sufficient proportions, consequently causing disastrous failures. Pipe weld lines such as girth welds and their adjacent heat affected zones are potential locations for micro-crack development, often caused by incomplete welds, porosities, and dents.

Pipeline codes such as API 570, API 1104 and DNV 96 have addressed various techniques as the accepted standard procedures for non-destructive inspection of pipelines. These include liquid penetrant testing (PT), magnetic particle testing (WFMT), ultrasonic testing (UT), magnetic flux leakage (MFL), and radiography testing (RT). However, the most conventional practices for inspection of girth welds in pipelines are generally radiography and ultrasonic techniques [1]. Although both methods, and specifically the latter, have been successfully and regularly practiced in most cases, they are expensive and require highly trained technicians for testing and result interpretation. Furthermore, radiography testing has relative insensitivity to sharp flaws such as cracks [2], and

[1] Address for correspondence: 1360 Barrington Street, Halifax, NS, B3J 1Z1, Canada.

ultrasonic testing has difficulties in dealing with non-straight welds, non-constant width, and misalignment of the inner and outer beads [3].

Structural health monitoring via modal characteristics is an emerging category of damage detection that has received attention by many researchers in recent years. These methods rely on the fact that the occurrence of damage in a structure can be tracked through the deviations that can be detected within the structure's dynamic properties. Modal parameters, such as natural frequencies/mode shapes [4], modal strain energy [5], structural stiffness [6], etc, have all been studied as damage sensitive features with different degrees of success. There is an extensive amount of research dedicated to crack identification in various systems, such as beam-like structures, using modal properties [7–9]. However, few studies have been published regarding crack diagnosis in pipelines via dynamic properties assessment. One study was reported by Srinivasan and Kot [10], in which the feasibility of assessing damage (in form of a circumferential notch) in a thin circular cylindrical shell was assessed by measuring the changes in the dynamic characteristics. This study indicated that the natural frequencies and damping ratios were almost insensitive to the damage while certain mode shapes were affected by the damage. In another study, Wake and Evans [11] investigated the possibility of detection of annular cracks in gas cylinders by using the first few natural frequencies associated with the axi-symmetric modes. They concluded that annular cracks can be identified through relative changes in the natural frequencies of selected vibration modes. It was also stated that the reduction in natural frequencies of the axi-symmetric modes was approximately proportional to the square of the depth to wall thickness ratio of the crack.

In practical applications, modal damage detection methods have been addressed with some drawbacks in terms of their sensitivity to boundary conditions, sensor spacing, environmental effects such as temperature and moisture, and nonlinearities [12]. Moreover, dynamic based diagnosis methods provide information about the general health of the structure and are not well suited for the detection of small flaws, such as cracks, due to their insignificant contribution, in general, to the dynamic behavior of the structure. To overcome these disadvantageous aspects, other techniques, referred to as local diagnosis methods, have emerged, in which certain sensors/actuators, such as piezoceramics sensors, are placed adjacent to the damage to monitor the local failure modes in the structure. For instance, Tua *et al* [13] used an array of piezoceramic sensors/actuators to detect micro-width cracks on an aluminum plate and also on a pipe with the help of Lamb waves excited at frequencies about 600 kHz. Although this method could successfully detect the micro-cracks, it required a large number of sensors/actuators in order to scan the whole area of interest in the structure.

Another developing category of non-destructive testing using dynamic data is to employ time-series analyses. In these methods, the vibration signals are analyzed through signal processing techniques, such as the Fourier transform or wavelet analysis, with the purpose of extracting some damage sensitive features within the processed and decomposed data. For instance, Krawczuk [14] introduced an optimization process based on a genetic algorithm for the detection of small cracks in beams using a Fourier transform of the dynamic responses of the structure in conjunction with finite element data. In addition, Quek *et al* [15] examined the distribution of wavelet coefficients of the beam deflection profiles, for which sudden changes were proposed as a crack indicator.

A new time-series analysis, known as the Hilbert–Huang transform (HHT), was recently introduced by Huang *et al* [16] and has received significant attention for its use in structural health monitoring applications. The HHT is an adaptive signal processing technique that produces signal decomposition in time and frequency domains, thus providing valuable information, such as instantaneous frequencies, phase, and damping, that can be used for damage detection purposes. This method has been successfully applied for damage diagnosis in building structures [17, 18]. Moreover, Cheraghi *et al* [19, 20] employed the decomposition part of the HHT, known as the empirical mode decomposition (EMD), and proposed a damage index called the 'EMD energy damage index' for structural health monitoring, and verified its applicability through numerical and experimental studies. The proposed method utilizes an energy term obtained from EMD and compares the healthy and damaged states of the structure. The applicability of the EMD energy damage index was further experimentally investigated by Rezaei and Taheri [21, 22] for detection and quantification of corrosion in pipelines. The results of these studies demonstrated the effectiveness of the proposed damage index for structural health monitoring applications.

In the present paper, the HHT, as a time-series analysis technique, has been combined with a local diagnosis approach in order to detect cracks and identify their severity in girth weld of pipelines. In the proposed methodology, certain sensors, such as piezoceramic sensors and laser Doppler vibrometers, were used to monitor the local vibration of the pipeline in the weld vicinity. The vibration data gathered for the healthy and damaged states of the pipe were then decomposed by EMD and processed by HHT. Afterward, the EMD energy damage index, as well as the instantaneous phase, was examined for crack identification. The applicability of the method has been numerically and experimentally verified by examination of a standard steel pipe damaged with a notch at the mid-span girth weld. The effect of internal pressure on the damage detection method was also studied.

It should be mentioned that the aforesaid methodology is not intended to replace current technologies such as ultrasonic inspection, which is able to detect very small cracks while the damage investigated in this paper is much greater. Ultimately, the main objective of the study documented in the this paper was to establish an economical and uncomplicated inspection method which may serve as an early warning system in practical applications before the crack reaches a critical size, thereby causing pipeline failure, an undesirable monitory and environmental consequence. It is believed that the proposed methodology could be beneficial in applications where the use of traditional inspection methods is unfeasible or uneconomical (such as in refineries, petrochemical plants

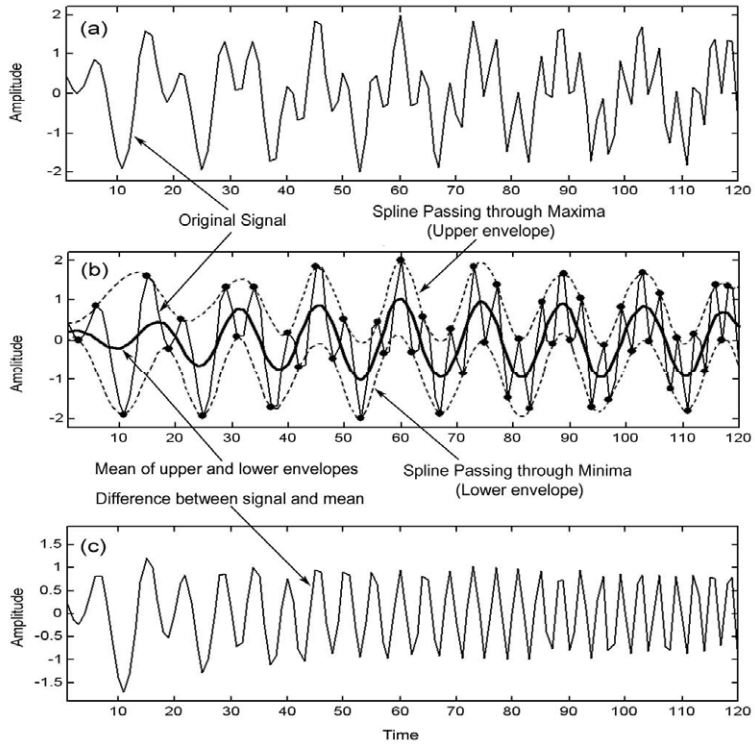

Figure 1. A schematic representation of the sifting process. (a) The original signal; (b) the original signal (in thin solid line); the upper and lower envelopes (in dot–dashed lines); the mean (in thick solid line); (c) the difference between the signal and mean.

and utility pipelines). Moreover, the proposed methodology could be used as the 'first line of defense', so as to lower the overall cost of inspection (e.g., in health monitoring of joints). In several practical cases, damage may occur in joints (whether welded or mechanically fastened) in which, based on the serviceability criterion, the component may be rendered as failed (e.g., a joint in a natural gas line). In such a case there would be no need for an elaborate investigation (e.g., the use of ultrasonic inspection, which may be significantly costly). In other cases (e.g., corrosion in a pipeline), the presence of damage may be monitored, with the proposed method, as the first line of defense, in which case a more elaborate method such as ultrasonic may be deemed necessary for further inspection and determination of the remaining useful life of the system.

2. Hilbert–Huang transform

In 1998, Huang *et al* [16] introduced a new adaptive signal processing method, referred to as Hilbert–Huang transform (HHT), which almost satisfied all the requirements for processing linear, nonlinear, stationary, and non-stationary signals. The HHT consists of two main parts: (i) EMD and (ii) Hilbert transform. The EMD method decomposes a real signal into a collection of simpler modes or intrinsic mode functions (IMFs), which are basically associated with energy of the signal at different timescales and contain important data characteristics [16]. The Hilbert transform, once applied to IMFs, produces an energy-frequency-time distribution of the data, known as a Hilbert spectrum. In general, the decomposition resulting from HHT is well localized in the time–frequency domain and reveals important information within its data.

The EMD employs a sifting process, as shown in figure 1, to extract the IMFs. To extract the IMFs for a given time signal, two cubic splines are fitted through the signal's local maxima and minima to produce an upper and lower envelope, respectively. The average of these two splines, or envelopes, is then subtracted from the original signal. The resultant signal is subsequently treated as the original time signal and the whole process, which includes the spline fitting, averaging, and subtraction, is repeated. At each step the sifting process produces a more symmetric signal with respect to the zero mean. To avoid removing the physically meaningful amplitude and fluctuations, Huang *et al* [16] proposed a stopping criterion for the sifting process. This criterion is based on limiting the size of the standard deviation (SD) computed from the last two successive sifting results. After the sifting process is stopped, the first IMF component of the signal is extracted. Each IMF must satisfy two conditions. Firstly, the number of extrema and the number of zero crossings are either equal or differ at most by one. Secondly, the average of the envelopes, defined by the local maxima and local minima, is zero. The first IMF component contains the shortest period component of the signal. To derive other IMFs, the first IMF is removed from the signal, the residue is considered as the new signal, and the sifting process is performed to obtain the second IMF component. This procedure is repeated for all subsequent residues to derive the longer period components. After extracting all IMFs, the original signal is decomposed

into n empirical modes, c_i, and a residue, r_n, which can either be the mean trend or a constant. This can be represented by the following mathematical relation:

$$X(t) = \sum_{i=1}^{n} C_i(t) + r_n(t). \tag{1}$$

For a more detailed description of the sifting process the reader is referred to the reference [16]. After extraction of IMFs through the sifting process, a Hilbert transform can be applied on each IMF in order to obtain the amplitude, phase and frequency data. For a given IMF $C_i(t) \equiv x(t)$, the Hilbert transform $y(t)$ is defined as the convolution of $x(t)$ and $1/(\pi\, t)$. The mathematical form of Hilbert transform is expressed as:

$$H[x(t)] = y(t) = \frac{1}{\pi} P \int_{-\infty}^{+\infty} \frac{x(\tau)}{t-\tau}\, \mathrm{d}\tau \tag{2}$$

where P indicates that the integral is to be considered as a Cauchy principal value, which prevents a possible singularity at $t = \tau$ and $\pm\infty$. When the Hilbert transform is applied on $x(t)$, the magnitude is kept unchanged but the phase of all frequency components is shifted by $\pi/2$. Using the Hilbert transform, an analytic signal $z(t)$ can be defined as the complex conjugate of $x(t)$ and its Hilbert transform $y(t)$ [16]:

$$\begin{gathered} z(t) = x(t) + \mathrm{i}y(t) = a(t)\, \mathrm{e}^{\mathrm{i}\theta(t)} \\ a(t) = \sqrt{x^2(t) + y^2(t)}; \qquad \theta(t) = \arctan\left(\frac{y(t)}{x(t)}\right) \end{gathered} \tag{3}$$

where $a(t)$ and $\theta(t)$ are called the amplitude and the instantaneous phase function of $x(t)$, respectively. Mathematically, the above polar expression provides the best local fit for any signal $x(t)$ with varying amplitude and phase [16]. Because the IMFs are symmetric with respect to zero mean, the instantaneous phase increases monotonically as a function of time.

In summary, processing vibration signals by EMD coupled with the Hilbert transform reveals significant fundamental information buried in the signals that can be utilized as damage sensitive features for structural health monitoring purposes. Depending on the structure being studied, a variety of information extracted from the HHT and EMD can be used. This information consists of intrinsic mode functions, instantaneous frequency, phase, amplitude, and damping. In this paper, the validity of a damage index known as the EMD energy damage index for crack detection in pipeline was examined. Furthermore, the instantaneous phase was also analyzed for crack identification. The following section details the EMD energy damage index.

The EMD energy damage index (EMD-EDI) introduced by Cheraghi *et al* [19, 20] is based on the energy of the vibration signal's first IMF. According to this method, the dynamic characteristics of the healthy structure during free vibration are collected through sensors; the acquired signals are then passed through a band-pass filter to ensure the existence of the first natural frequency within the data. This is followed by extraction of the first IMF though EMD. Finally, the energy of the first IMF for each sensor is established by:

$$E = \int_0^{t_0} (\mathrm{IMF})^2\, \mathrm{d}t. \tag{4}$$

The above procedure is repeated for the same structure in its damaged state to determine the energy of each signal's first IMF. The last step is the application of the EMD-EDI to each sensor:

$$\text{EMD-EDI} = \left| \frac{E_{\text{Healthy}} - E_{\text{Damaged}}}{E_{\text{Healthy}}} \right| \times 100. \tag{5}$$

Once EMD-EDI is calculated for each sensor, the existence and severity of damage may be determined by associating the high index values with the existence of damage close to the respective sensors.

Table 1. Material properties and dimensions of the steel pipe.

Dimension (mm)	Material property
Outside diameter: 168.3	E: 200 GPa
Wall thickness: 6.4	ν: 0.30
Length: 3685.0	ρ: 7860 kg m^{-3}

3. Numerical study

To illustrate the applicability of the HHT in structural health monitoring, a set of finite element (FE) simulations were conducted on a suspended pipe in order to detect a notch in the pipe girth weld. The pipe was an API compliant [23] standard steel with a girth weld at the mid-span. The pipe dimensions and material properties are listed in table 1. Different damage scenarios, including three notch locations (top, bottom, and side of the pipe) and three notch sizes at each location were studied. The notches were located adjacent to the weld on the left side. The depth of the first notch was $a/t = 0.3$ and its length was $L = 36.0$ mm (where a, t, L are as specified in figure 2). For the second notch, $a/t = 0.5$ and $L = 46.0$ mm, and for the third notch, $a/t = 0.7$ and $L = 56.0$ mm. The notch width was 0.35 mm for all cases. Table 2 summarizes the specifications of each damage case.

It is worth mentioning that the notch sizes studied in the present work were selected based on the guidelines given in DNV-RP-F108 [24]. This standard states that in pipeline girth welds '*the flaw sizes of interest are usually controlled by the weld pass height and are therefore relatively small, typically 2–6 mm in height*'. The weld pass height used in the experiment was measured to be 2.5 mm and, therefore, the minimum notch depth was chosen to be 2.0 mm. The other two notch depths (3.2 and 4.5 mm) were studied to examine the capability of the proposed damage detection method in following the progression of the damage due to service loading.

To monitor the dynamic response of the pipe, piezoceramic (PZT) sensors were modeled and placed circumferentially close to the girth weld on either side of the weld. The sensors are of type PZT-5H, available from Piezo Systems Inc. (Cambridge, MA, USA). The following matrices list

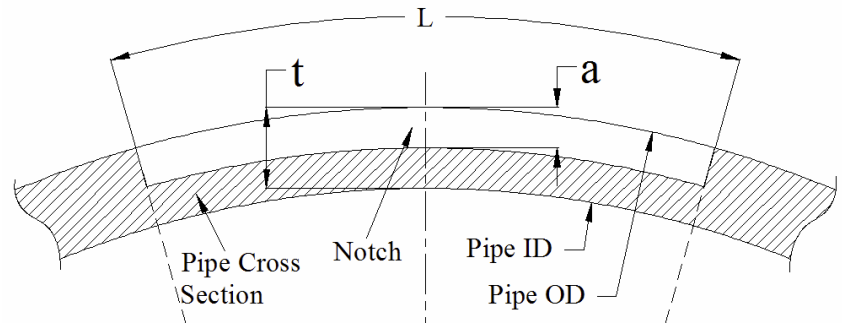

Figure 2. Schematic of the notch geometry used in the FE model.

Table 2. Description of different damage cases.

Damage case	Notch location	Notch depth (a/t)	Notch length in finite element L (mm)	Notch length in experiment L (mm)	Reference
DC1	Top (12 o'clock)	0.3	36.0	65.0	DC1-0.3
		0.5	46.0	75.0	DC1-0.5
		0.7	56.0	85.0	DC1-0.7
DC2	Side (3 o'clock)	0.3	36.0	65.0	DC2-0.3
		0.5	46.0	75.0	DC2-0.5
		0.7	56.0	85.0	DC2-0.7
DC3	Bottom (6 o'clock)	0.3	36.0	65.0	DC3-0.3
		0.5	46.0	75.0	DC3-0.5
		0.7	56.0	85.0	DC3-0.7

the material properties of the sensors obtained from the manufacturer. The density of PZT-5H is 7500 kg m^{-3}.

$$S_E[\mathrm{m^2\,N^{-1}}] = (10^{-12})\begin{bmatrix} 16.5 & -4.78 & -8.45 & 0 & 0 & 0 \\ -4.78 & 16.5 & -8.45 & 0 & 0 & 0 \\ -8.45 & -8.45 & 20.7 & 0 & 0 & 0 \\ 0 & 0 & 0 & 43.5 & 0 & 0 \\ 0 & 0 & 0 & 0 & 43.5 & 0 \\ 0 & 0 & 0 & 0 & 0 & 42.6 \end{bmatrix}$$

$$d[\mathrm{C\,N^{-1}}] = (10^{-12})\begin{bmatrix} 0 & 0 & 0 & 0 & 741 & 0 \\ 0 & 0 & 0 & 741 & 0 & 0 \\ -274 & -274 & 593 & 0 & 0 & 0 \end{bmatrix};$$

$$\varepsilon^S[\mathrm{F\,m^{-1}}] = (10^{-9})\begin{bmatrix} 27.7 & 0 & 0 \\ 0 & 27.7 & 0 \\ 0 & 0 & 30.1 \end{bmatrix}$$

where S_E is the compliance matrix, d is the piezoelectric coupling matrix, and ε^S is the permittivity of the piezoceramic.

The commercial FE code Abaqus 6.8 (Dassault Systemes Simulia Corp., Providence, RI, USA) was used to simulate the response of the pipe and the piezoceramic sensors. The pipe was modeled using C3D8R, Abaqus's 8-node linear brick element with reduced integration and hourglass control and for the piezoceramic sensors, the 8-node linear piezoelectric brick (C3D8E) was used. The discretization of the pipe was executed such that, in regions adjacent to the weld and PZT sensors, a fine mesh was used in order to accurately capture the local vibrations of the pipe. The mesh size was correspondingly increased in other areas to reduce the computation costs. In order to take into account the local stiffening due to the weld, a bulge of 15.0 mm wide and 2.5 mm high was modeled over the pipe at the weld location (see figure 3). For modeling the notch, a U-shape notch with a width of 0.35 mm was created at the desired location (figure 2) and the mesh was refined within the notch proximity. Figure 3 illustrates the FE model of the pipe as well as the PZT sensor numbering. As shown, sixteen PZT sensors were located at a distance of 6.0 mm from the weld, with eight sensors (LPZT1 through LPZT8) at the left and eight sensors (RPZT1 through RPZT8) at the right side of the girth weld. The sensors were 25.0 mm long, 10.0 mm wide and 1.0 mm thick.

From the standpoint of fracture mechanics, the presence of a notch introduces singular stresses and strains at the notch tip that are functions of $\frac{1}{\sqrt{r}}$, where r is the distance from the notch tip. To model this singularity, special elements known as singular elements are usually used to model the notch tip. These elements are quadratic with the mid-side nodes placed at the quarter points. However, in the present study, the local changes in the vibration pattern of the pipe due to local loss of stiffness are considered, rather than the variation in stress or strain fields at the tip of the notch. A comparison of the natural frequencies of a notched beam when the singular elements are used, and when they were not used, was presented in a paper by Chati *et al* [25]. In this paper, it was concluded that the frequencies for both cases were quite close. Consequently, the dynamic behavior of the beam can be accurately simulated without using the singular elements, provided that the mesh is refined adjacent to the notch.

At this stage of our investigation, it was decided to use free–free boundary conditions for the pipe setup. This was done to simulate the response of real on-shore over-ground pipelines, which are used for energy transfer in long distances all over the world, as well as in refineries, petrochemical

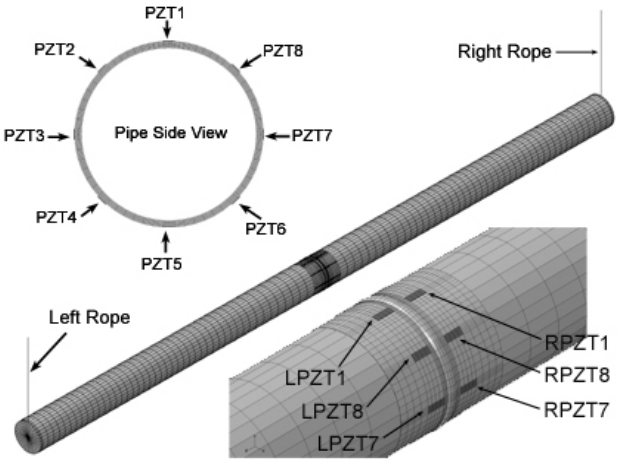

Figure 3. FE model of the pipe with the girth weld and the arrangement of the PZT sensors.

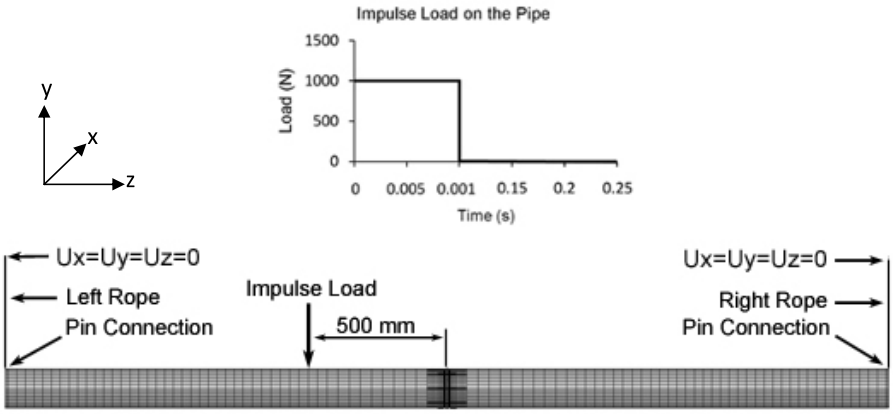

Figure 4. FE model of the pipe depicting the boundary conditions and loading function.

plants and several large scale physical plants. Furthermore, free–free boundary conditions reduce the effect of boundary conditions on the pipe dynamics. Thus, a suspended pipe was considered such that the pipe was hanging at its both ends by nylon ropes. The ropes were modeled using 2-node 3D linear beam elements (B31). The free end of the ropes were fixed in the x, y, and z translations and, at the left and right attachment points of the pipe ends and the ropes, a pin joint was established using the multipoint constraint capability in Abaqus. Figure 4 illustrates the boundary conditions of the pipe. To study the free vibration of the beam, an impulse load was applied on the pipe at a distance of 500.0 mm from the weld on the left side of the weld. The magnitude of this load was 1000 N and its duration was 0.001 s. The loading function and the impact location on the pipe are depicted in figure 4. A transient analysis of the beam was conducted in Abaqus to simulate the free vibration response of the beam due to the impulse load. Newmark's integration scheme was employed as the solver, and the time increment was kept fixed at 0.0001 s. After applying the impulse load, the free vibration of the beam was calculated up to 0.25 s.

To insure the validity of the FE model and the transient simulation, the first few natural frequencies of the pipe were calculated from the output voltage of the PZT elements, and then compared with the analytical values. This comparison indicated that the FE model and the transient analysis were reasonably accurate in simulating the dynamic behavior of the pipe. After verifying the FE model, a transient analysis was performed for the un-notched pipe as well as for the notched pipe for each damage case. Knowing the sensor voltages for the un-notched pipe and the notched pipe at each damage case, the empirical mode decomposition was used, along with the EMD energy damage index given by equation (5), to assess the damage. For this purpose, a MATLAB code was developed in-house to decompose the voltage signals based on the EMD method, to derive the IMFs, and to calculate the energy of the first IMF for each sensor.

Cheraghi *et al* [19, 20] suggested a band-pass filtering of data in order to retain only the first frequency. In the present study, the signals were filtered with various band widths and it was concluded that a band-pass filter with a pass band frequency of 2000–3000 Hz would give the best resolution for the damage index. This can be explained by the fact that small damages such as cracks are usually associated with higher frequency components. Moreover, a study of the frequency components of the pipe using Fourier analysis revealed that two frequency ranges had the greatest amplitude. The first range from 0 to 1200 Hz had the greatest

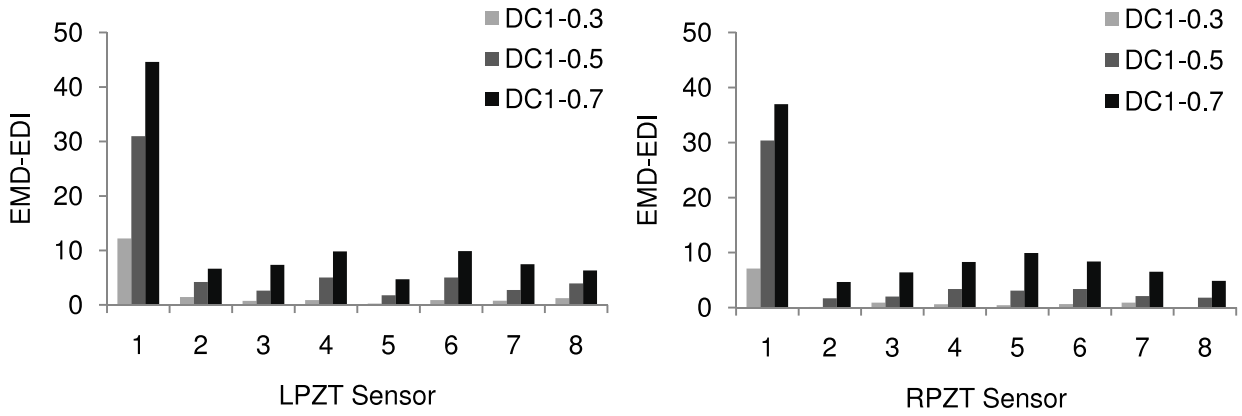

Figure 5. EMD-EDI evaluated from the first IMF of the PZT sensors for the unpressurized pipe with a top notch simulated by the FE method.

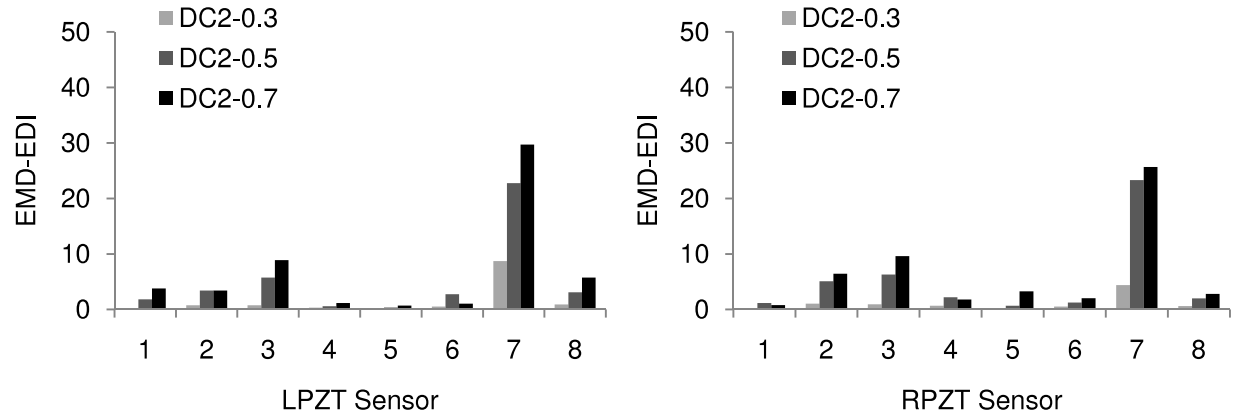

Figure 6. EMD-EDI evaluated from the first IMF of the PZT sensors for the unpressurized pipe with a side notch simulated by the FE method.

amplitude, whereas the amplitude of the second range, 2000–3000 Hz, was approximately half of the first range. The amplitudes at other frequency ranges were much lower than the above-mentioned bands. It is believed that the first high amplitude frequency set is not sensitive to the notch, since it only contains the low frequency components. Consequently, it is the second set that is influenced by the notch. Furthermore, if only frequencies between 0 and 3000 Hz were considered the frequency components in the first range would have noticeably reduced the resolution of the damage index due to their high amplitude, which significantly undermines the contribution of other frequency components in the pipe dynamics. Thus, band-pass filtering used in the application of the EMD-EDI for notch or crack detection should be carefully implemented in order to only take into account the frequency components that are sensitive to the damage.

4. Numerical results and discussion

For the case of the pipe with no internal pressure, figures 5–7 illustrate the EMD-EDI obtained from all PZT sensors for the first, second, and third damage case, respectively. From these figures it can be clearly observed that for all damage cases, the EMD-EDI calculated from most of the sensors could successfully detect the presence of damage and, more interestingly, could indicate the progression of damage. It can also be inferred that for each damage case the sensors with closer proximity to the damage showed the highest sensitivity. These sensors were LPZT1 and RPZT1 for the first damage case, LPZT7 and RPZT7 for the second damage case and LPZT5 and RPZT5 for the third damage case. For the first and second damage cases, the other sensors showed a relatively low sensitivity to the damage presence. However, for the third damage case, LPZT4, RPZT4, LPZT6 and RPZT6 all had high amplitude damage indices. These four sensors were at an angle of 45° from PZT5 (see figure 3). This is a promising observation for practical applications, since girth weld cracks can occur in any location along the weld; however, they are most often found at the bottom and inside of pipes [26]. This is mainly due to the existence of maximum stresses induced in this area during both construction and service. Consequently, the FE results indicate that damage located at 6 o'clock can be detected by having only one sensor located in the region along 4–8 o'clock.

Considering the amplitude of the EMD-EDI in figures 5–7, the notch on the top produced the greatest amplitude and the notch on the bottom generated the second greatest amplitude, while the notch on the side had the lowest amplitude. This can be explained by the fact that a notch on the top or bottom of the pipe would have a greater contribution to the flexural stiffness

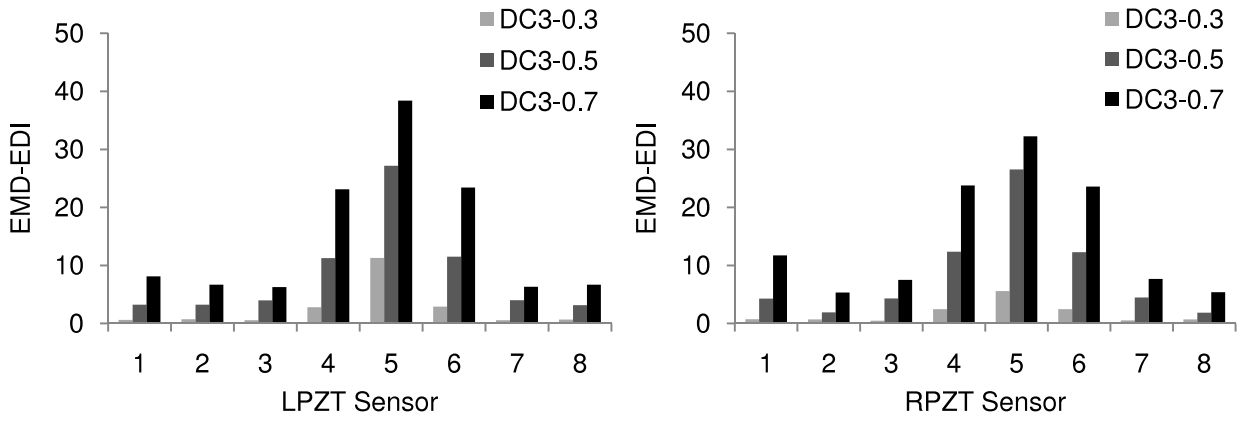

Figure 7. EMD-EDI evaluated from the first IMF of the PZT sensors for the unpressurized pipe with a bottom notch simulated by the FE method.

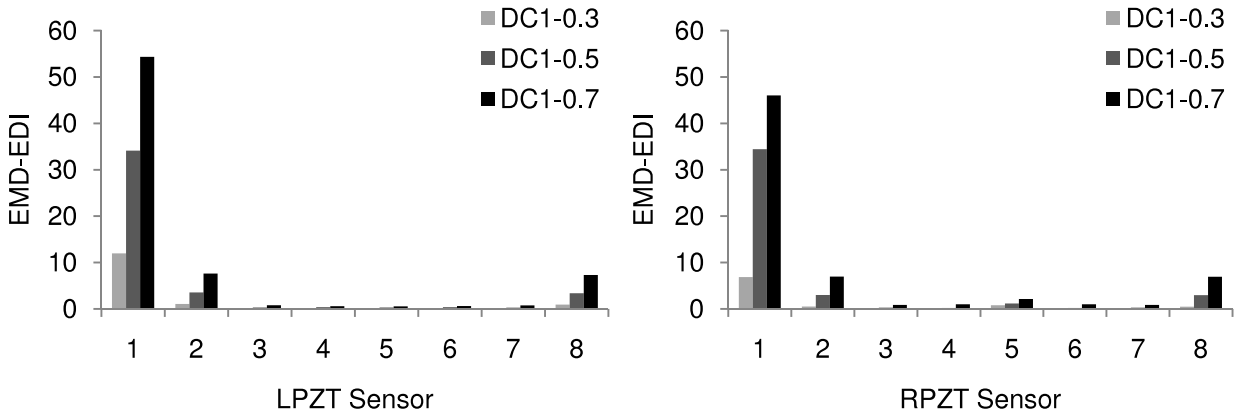

Figure 8. EMD-EDI evaluated from the first IMF of the PZT sensors for the pressurized pipe with a top notch simulated by the FE method.

of the pipe, as opposed to a notch on the side, which is located on the neutral axis of the pipe.

Referring to figures 5–7, it is obvious that for all damage cases the sensor closest to the notch at the left side of the weld has produced higher amplitudes of EMD-EDI than the sensor on the right side of the weld. This is due to the fact that the sensor to the left of the weld is closer to the notch and therefore more responsive to the damage. Furthermore, the pipe is impacted at the left side and the vibration has to pass through the weld to reach the right sensor.

In general it can be concluded that the EMD-EDI can detect damages in different locations in the girth weld and identify their severity qualitatively. Moreover, the sensor closest to the damage showed the highest sensitivity while the other sensors did not demonstrate any noticeable sensitivity to the damage. However these results were all achieved for an unpressurized pipe, while in real applications pipelines are used to transfer chemicals which are normally pressurized. Therefore, the pipe will be under an internal pressure which can appreciably affect the pipe dynamics.

The influence of the internal pressure on the vibration characteristics of cylinders has been investigated by Fung *et al* [27] and Yong *et al* [28]. In both studies it was observed that, in thin cylinders, the internal pressure would have a significant effect on the natural vibration characteristics, and that the frequencies would increase in the presence of the internal pressure. Fung *et al* [27] also concluded that the rate of change in the fundamental frequency would be faster at lower internal pressures. Another observation made by Yong *et al* [28] was that the effect of internal pressure on frequencies for a higher circumferential mode was more significant than for a lower circumferential mode.

Based on the above observations, the capability of the EMD-EDI for notch detection in pipes under internal pressure had to be numerically studied. For this purpose, all the FE simulations implemented on the unpressurized pipe were repeated for a pipe with an internal pressure of 10 MPa. This pressure is believed to be the normal operating pressure in oil/gas pipelines. The pipe material and geometry were identical to the cases for the unpressurized pipe. The EMD-EDI results obtained from the PZT sensors for the different damage cases on the pressurized pipe are depicted in figures 8–10. Similar to the unpressurized pipe, one can observe that for each damage case the closest sensor to the notch shows the highest sensitivity to the damage. The damage progression for each case has also been successfully detected. In contrast to the closest sensor to the notch, the adjacent sensors at 45° from either side of the notch showed small values of

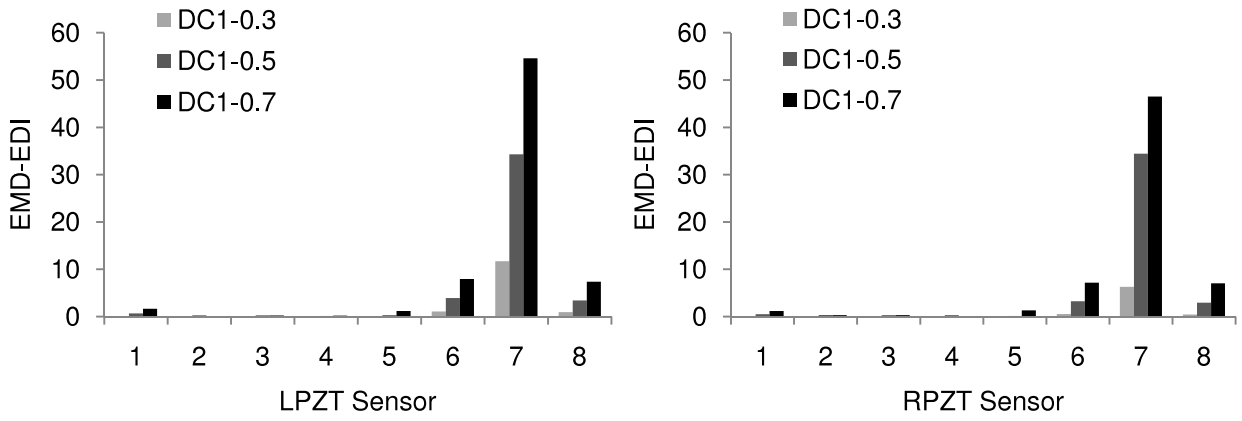

Figure 9. EMD-EDI evaluated from the first IMF of the PZT sensors for the pressurized pipe with a side notch simulated by the FE method.

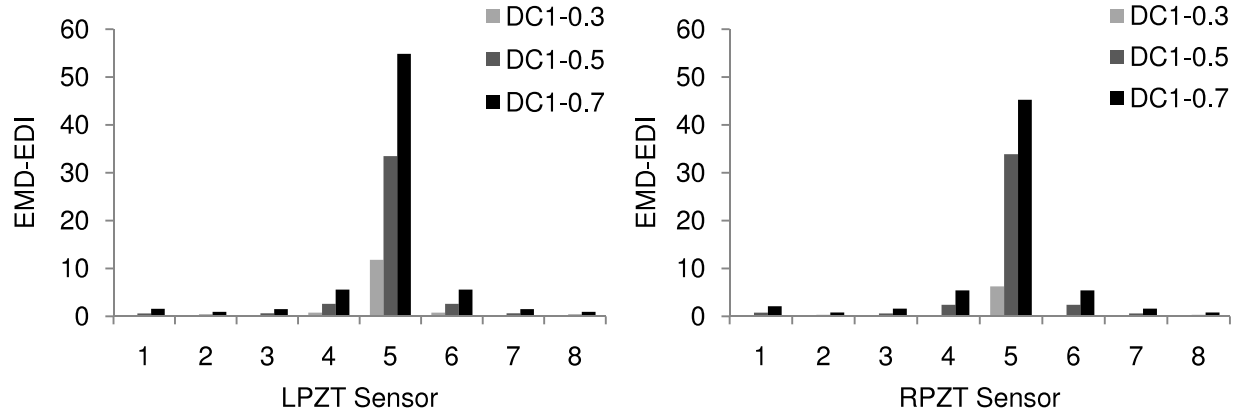

Figure 10. EMD-EDI evaluated from the first IMF of the PZT sensors for the pressurized pipe with a bottom notch simulated by the FE method.

the EMD-EDI, and the other sensors were almost insensitive to the damage. Another observation is that for each notch depth, the EMD-EDI amplitude of the closest sensor to the notch is almost the same for the top, side and bottom notches. Furthermore, by comparing the results for the unpressurized and pressurized pipes it can be inferred that the latter produces higher amplitudes of EMD-EDI for the closest sensor to the notch. Therefore, it can be concluded, in general, that not only could the EMD-EDI successfully identify the presence of damage and its severity in pipes under internal pressure, but the resolution of damage detection was also improved in comparison to the unpressurized pipe.

After successful utilization of PZT sensors coupled with the EMD-EDI, the applicability of other vibrational signals, such as velocity, was also studied for structural health monitoring. In practice, the vibrational velocity of structures can be measured by a laser Doppler vibrometer (LDV). In the FE analysis, in order to simulate the data from LDV, the velocity (in the normal direction to the pipe surface) of certain nodes located halfway between the PZTs and the girth weld was extracted. The velocity signal was obtained for the intact pipe as well as for the notched pipe for each damage scenario as listed in table 2. The EMD-EDI values calculated from the velocity signals of the pressurized pipe are depicted in figures 11–13. One should note that the results produced from the unpressurized pipe analysis were similar to those from the pressurized pipe.

From figures 11 to 13 it can be seen that for all damage cases the EMD-EDI calculated from the velocity at the closest location to the notch identifies the damage with the best resolution. These are locations 1, 7, and 5 for the top, side, and bottom notch cases, respectively. For the top and side notches the damage indices obtained from the velocity signals at the other locations are not significant. However, for the bottom notch, the EMD-EDI values at the three closest locations (4, 5, and 6) are relatively high, with the greatest amplitude observed at location 5.

Another observation from figures 11 to 13 is that among the damage indices obtained for the top, side and bottom notches, the indices for the side notch are the highest and those for the top are the lowest. In contrast, the damage indices calculated from the PZT sensors' signals were approximately the same for all the notch locations. This is believed to be due to the fact that the PZT sensors are basically measuring the values of strain in the notch vicinity. In the higher vibration modes (i.e., both flexural and circumferential modes in nature) the notches located at different locations would experience similar strain patterns and therefore result in similar deviations as registered by the PZT sensors. In contrast, a LDV measures the velocity in the normal direction to the pipe's surface;

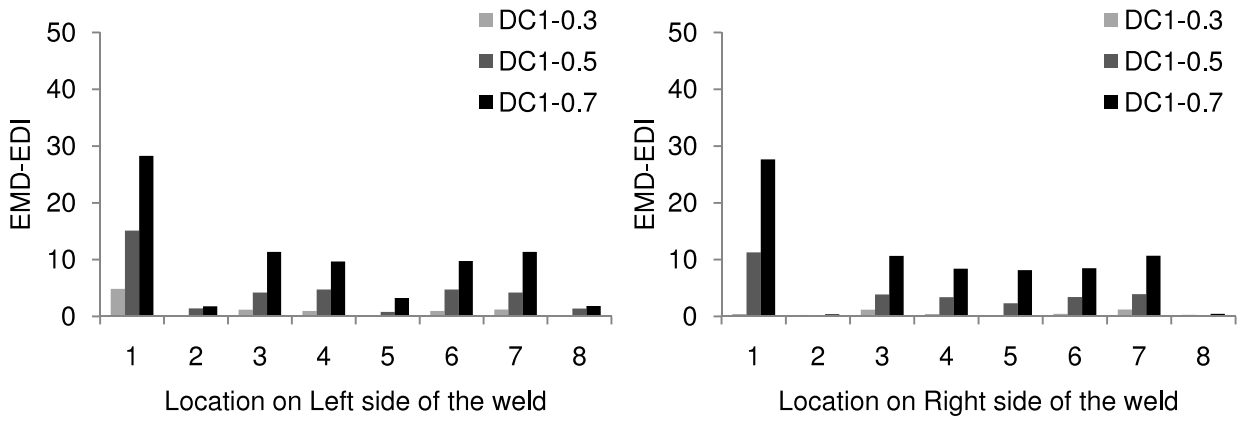

Figure 11. EMD-EDI evaluated from the first IMF of the velocity signals for the pressurized pipe with a top notch simulated by the FE method.

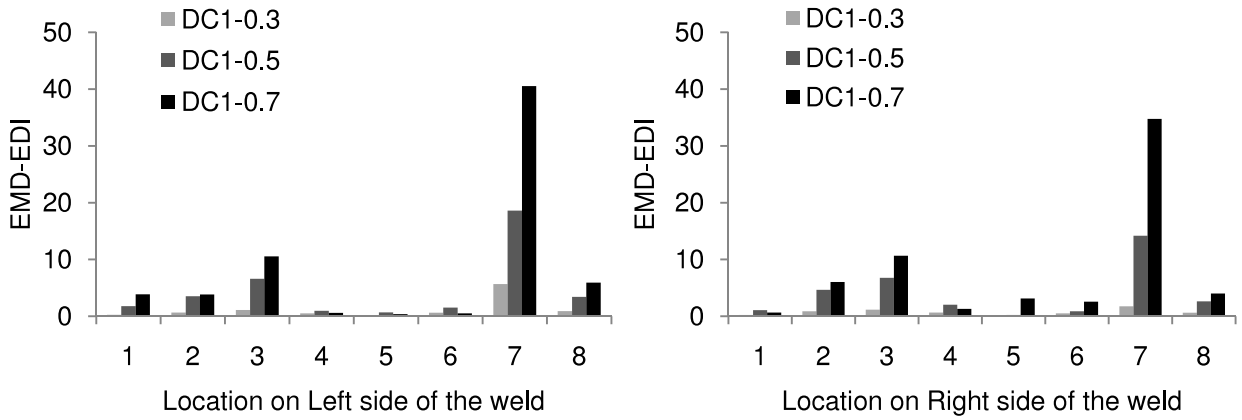

Figure 12. EMD-EDI evaluated from the first IMF of the velocity signals for the pressurized pipe with a side notch simulated by the FE method.

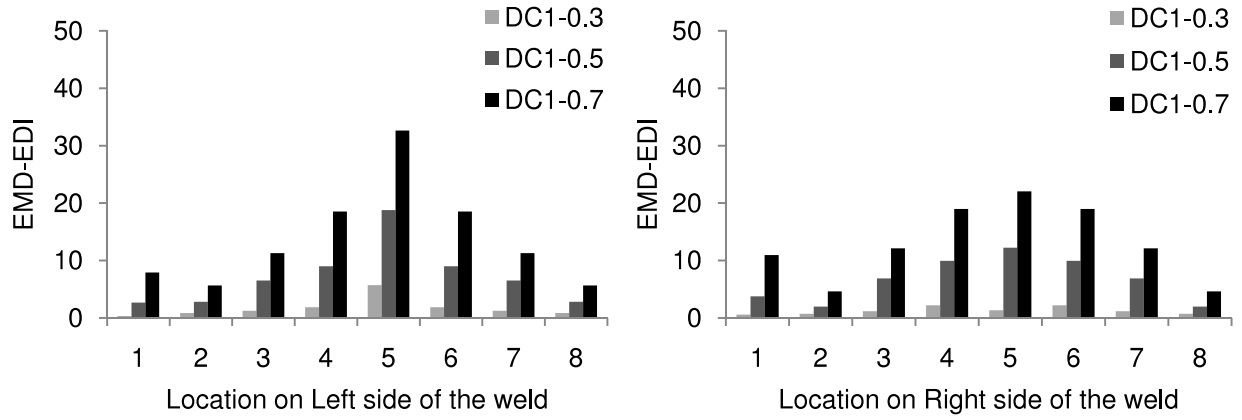

Figure 13. EMD-EDI evaluated from the first IMF of the velocity signals for the pressurized pipe with a bottom notch simulated by the FE method.

therefore, the simulated LDV data by the FE analysis expressed the same normal quantity at each location. Consequently, at each notch location, the velocity components present in other directions (i.e., tangential and axial) are ignored and, as a result, the impact of the notch on the velocity would be different at each notch location in comparison to the strain values measured by the piezoelectric sensors.

5. Experimental study

After obtaining the encouraging results from the FE simulations, the application of the EMD-EDI was examined experimentally on a standard steel pipe. The test specimen was the same pipe analyzed numerically (see table 1). Figure 14 depicts the experimental setup used in this study. As in the

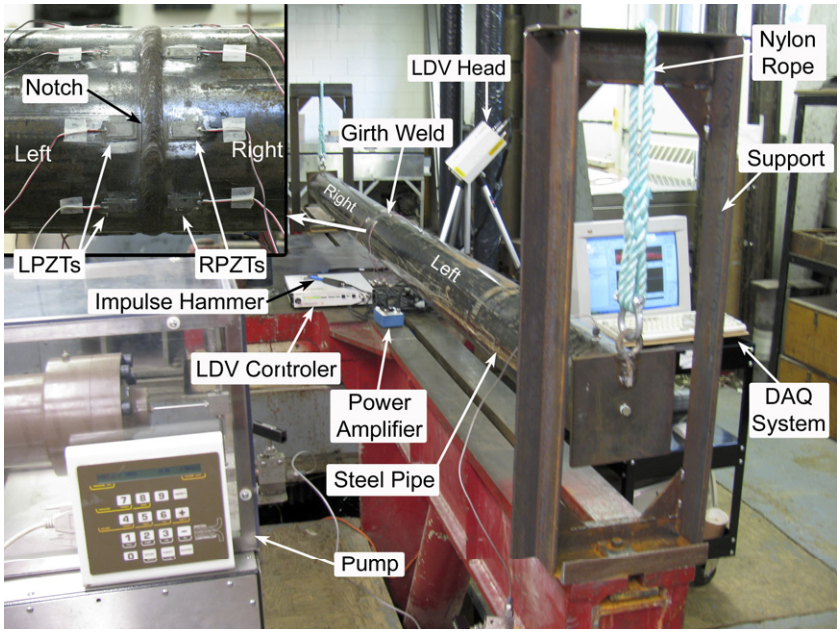

Figure 14. Experimental setup of the suspended steel pipe.

case of finite element simulation, the pipe was suspended from two supports using nylon ropes. To monitor the dynamic response of the pipe, sixteen PZT sensors were bonded at a distance of 6.0 mm from the weld, with eight sensors (LPZT1–LPZT8) at the left and eight sensors (RPZT1–RPZT8) at the right side of the girth weld. The numbering of the PZT sensors was identical to the FE simulations (see figure 15 and the inset of figure 14). The sensors were of type PZT-5H, available from Piezo Systems Inc. (Cambridge, MA, USA). The material properties and dimensions of the sensors were the same as those used in the numerical study. To attach the sensors, the pipe surface was cleaned using sandpaper and isopropyl alcohol. The PZT sensors were subsequently bonded to the pipe using a two part epoxy, Araldite 2011 (Huntsman Advanced Materials Americas Inc., Los Angeles, CA, USA), and secured firmly for 12 h to achieve a strong bond.

Figure 14 also demonstrates a laser Doppler vibrometer (LDV) which was used for measurement of the vibrational velocity. The LDV monitors the velocity of a vibrating object through the frequency shift between the laser beam projected to the object and the reflected beam. The LDV is able to monitor vibrations with a high degree of accuracy, sensitivity, and resolution. The LDV used in this study was a single beam LDV and, therefore, for measuring the vibration of each location the LDV had to be moved to that location. Due to access limitation, only six locations were chosen for LDV measurement, as illustrated in figure 15. As shown in figure 15, L1L and L1R are located at the top of the pipe between LPZT1 and the weld and RPZT1 and the weld, respectively. L8L and L8R are located between LPZT8 and the weld and RPZT8 and the weld, respectively. Similarly, L7L and L7R are located at the side of the pipe between LPZT7 and the weld and RPZT7 and the weld, respectively.

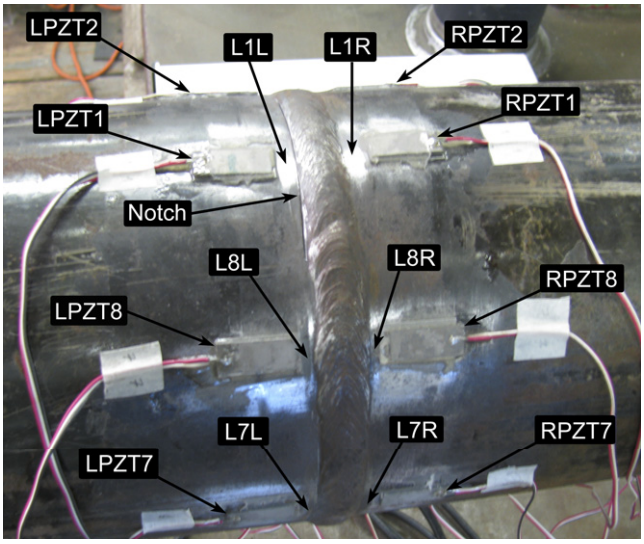

Figure 15. Locations for the LDV measurement: L1L, L1R, L7L, L7R, L8L, L8R.

To observe the pipe's free vibration, the pipe was excited with a piezoelectric impulse hammer (model 5800B5, Dytran Instrument Inc., Chatsworth, CA, USA) equipped with an aluminum tip. Similar to FE simulations, the pipe in the experimental study was also tested under unpressurized and pressurized conditions. To induce internal pressure, both ends of the pipe were sealed by welding two steel plates. The pipe was filled with water and then an electrical pump was used to apply the desired pressure in the pipe (see figure 14). In this study a pressure of 10.0 MPa was used for all cases.

To create the notch, a 0.35 mm wide notch was carefully cut into the pipe with a jeweler saw. After performing the

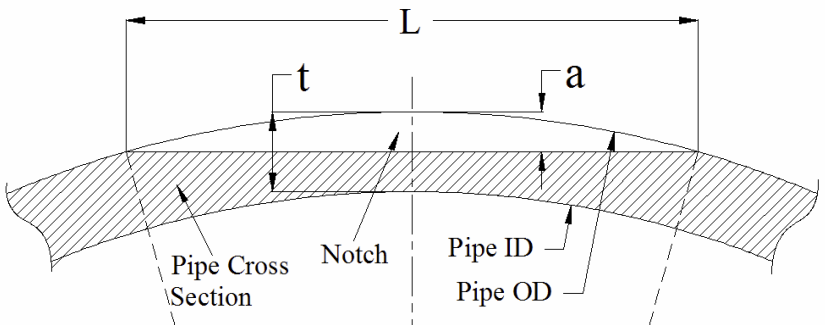

Figure 16. Schematic of notch geometry used in experiments.

vibration test on each notch size, the notch was cut to a deeper level to simulate the next notch depth for the next damage case. Figure 15 and the inset of figure 14 illustrate the notch at a depth 4.5 mm on the top of the pipe. Similar to the FE analysis, different damage scenarios were studied with three notch locations (top, bottom, and side of the pipe) including three notch sizes at each location. The depth of the notches was the same as those used for the FE simulations. However, due to practical limitations, the notch created by the jeweler saw had a different shape from the FE modeling. Refer to figure 16 to see the specification of the notch created experimentally and to table 2 for the notch dimensions and different damage scenarios. As listed in table 2, for the first notch, $a/t = 0.3$ and $L = 65.0$ mm, for the second notch, $a/t = 0.5$ and $L = 75.0$ mm, and for the third notch, $a/t = 0.7$ and $L = 85.0$ mm.

In regards to the different notch geometries used in FE models in comparison to that in the experiments, it should be noted that the numerical and experimental studies were carried out to demonstrate the capability of the proposed EMD-based damage detection method in identifying the damage and its qualitative severity. While the objective of the experimental study was to further demonstrate the validity of the proposed method when applied to real systems, the main purpose of the finite element investigation was to take advantage of the versatility of the finite element method to also demonstrate that the methodology works for different shape flaws. It should also be noted that consistent in both studies, the condition of the damaged system was compared to the healthy state of the system. In other words, the results obtained from the actual pipe with notches were compared to the actual pipe's response in its healthy state, and in the same vein, the simulation results of the notched pipes considered by FE were compared to the simulation results of the same pipes in their healthy state. So, the purpose was not comparing the real pipe response with the FE simulated system. It should be further emphasized that a parametric study of different notch lengths with FE simulations indicated that, so long as the notch depth is constant, variation in the notch length (for example: from 20 to 40 mm in the case of the top notch) would not have a noticeable effect on the calculated EMD energy damage index.

During the experiments, the response of the PZT sensors and the impulse hammer were concurrently collected through a multifunction PCI 6220 data acquisition card manufactured by National Instruments Inc. (Austin, Texas, USA). During testing, however, the DAQ System could only hold up to 8 inputs, and since the concurrent input from the impulse hammer was required as well, only 7 of the 8 PZT sensors were monitored. It was decided that LPZT3 and RPZT3 would be ignored due to the fact that they were the farthest sensors from the notch location. Consequently, for each case study the experiment was performed twice, once for acquiring data from the LPZTs and then for the RPZTs.

For velocity measurements, the LDV beam was targeted at the desired location, and the output voltage of the LDV and the impulse hammer were simultaneously acquired by the DAQ system. This experiment had to be repeated six times to complete data acquisitions at all six locations, since the LDV was a single beam LDV. During all experiments, the sampling frequency was kept at 10.0 kHz. A MATLAB code was also developed in-house to read the data produced by the DAQ system and then to process the response of the PZT sensors, LDV and impulse hammer. The code removes unwanted data before impact, filters the noise, compensates for any offset, normalizes the response of sensors, and analyzes the data by EMD and HHT.

In order to achieve consistent results for each case, the pipe was impacted five times and the acquired signals were normalized based on the input force (hammer signal). The degree of consistency in the difference between signals after normalization was deemed to be a good measure of the repeatability of the impact procedure. Next, the closest three signals out of the five were selected and, after processing by EMD or HHT, their average was chosen. With this procedure the maximum difference in the calculated parameters from the chosen signals was mostly below 5%, and in few cases was between 5% and 10%.

According to the procedure of the EMD-EDI technique, the free vibration of the intact pipe was initiated by impacting it using the impulse hammer, and the voltages of the impulse hammer and PZT sensors, or the LDV, at different locations were subsequently acquired by the DAQ system. A typical voltage signal (from sensor LPZT1) and its decomposition, based on the EMD sifting process, is illustrated in figure 17. After evaluating the healthy state of the pipe, a notch was created at the desired location on the pipe and the experiment was repeated to assess the damaged state of the pipe at that certain damage case. Afterward, the notch was cut deeper,

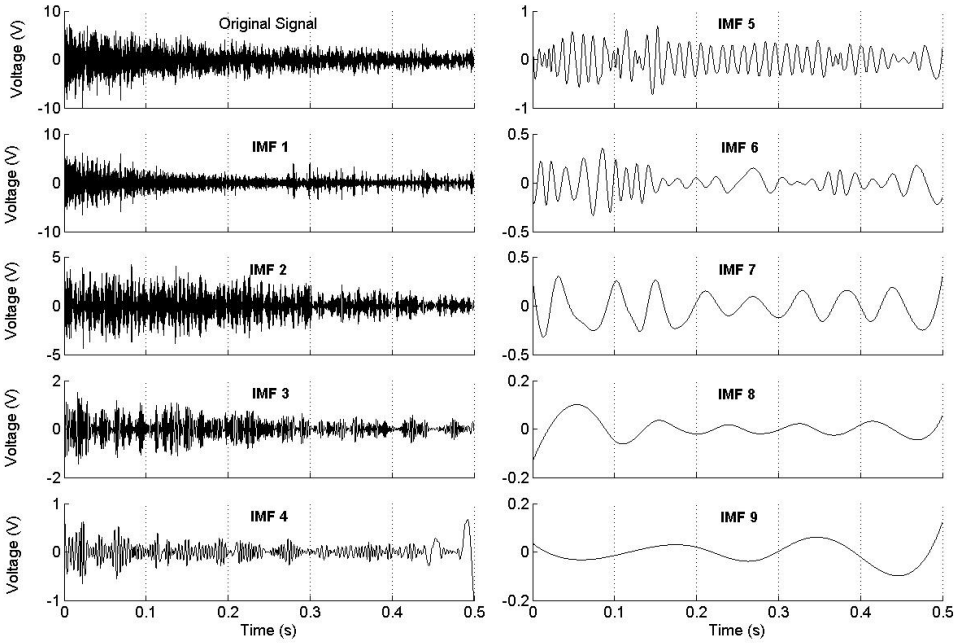

Figure 17. Typical signal of PZT1 and its first nine IMFs resulting from the EMD.

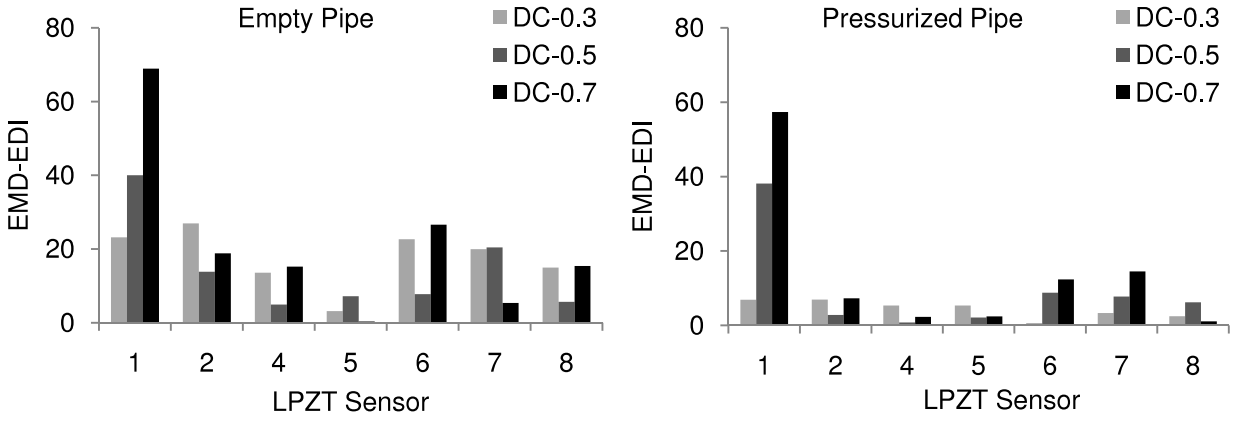

Figure 18. Experimental EMD-EDI evaluated from the first IMF of the PZT sensors for the pipe with a top notch.

to simulate the next damage case, and the experiment was repeated. After collecting the vibration signals of the pipe in its healthy and each damage case, the data was processed and analyzed by the EMD. Consequently, the deviations of energy of the first IMF between the healthy and damaged states were used to indicate the damage.

Based on the EMD-EDI, the damage index is based on the comparison of certain measures before and after the existence of damage. Therefore, there is no limitation in choosing the duration of signals so long as the same duration is used for processing the signals of the pipe in its un-notched and notched states. Thus, in the present work, only the first 0.5 s of the signals was considered for evaluation of the pipe's healthy state. It should be mentioned that, based on the results of the numerical study, a band-pass filter with a band frequency of 2.0–3.0 kHz was used in evaluating the damage indices in all experiments.

6. Experimental results and discussion

6.1. Experimental EMD-EDI results based on the first IMF

Figures 18–20 illustrate the EMD-EDI results obtained from the first IMF of the LPZT sensors for the different damage scenarios studied on the unpressurized and pressurized pipes. The pipe with the bottom notch was not tested under the pressurized condition and, therefore, no result is reported for this case. It can be seen that for all notch locations and notch severities, the closest LPZT sensor to the notch has produced the best resolution for the identification of damage. These sensors are LPZT1, LPZT7, and LPZT5 for damage located at the top, side and bottom of the pipe, respectively. Moreover, in all notch cases, the EMD-EDI at the aforementioned sensors follows a rising trend as a function of damage depth and length. This ascertains the effectiveness of the EMD-EDI in qualitative determination of damage severity.

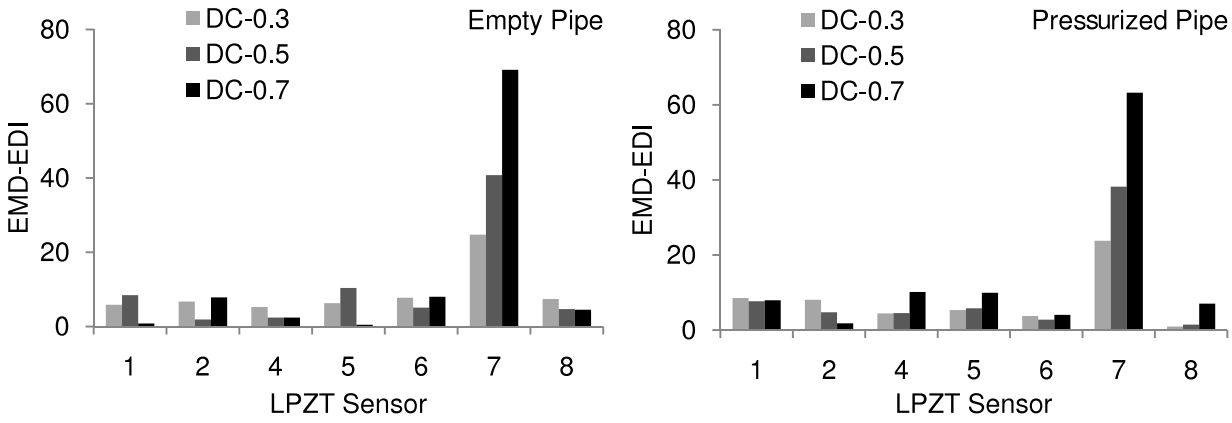

Figure 19. Experimental EMD-EDI evaluated from the first IMF of the PZT sensors for the pipe with a side notch.

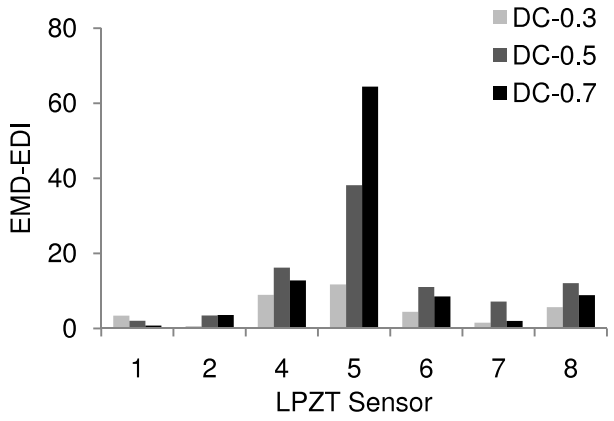

Figure 20. Experimental EMD-EDI evaluated from the first IMF of PZT sensors for the unpressurized pipe with a bottom notch.

The comparison of the experimental data with numerical results shown in figures 18–20 reveals that, in general, the experimental damage indices are larger than their numerical counterparts. This could be due to two factors: (a) in general, the finite element method's results are stiffer than that of real structures, and (b) the notch geometry in the experiments was slightly different from that used in the FE simulations (see figures 2 and 16).

Considering figures 18–20, two other observations can be made concerning the sensors that are far from the notch. To begin with, these sensors poorly identified the notch, so that the EMD-EDI obtained from these sensors was generally small; in most cases the highest registered value was less than 10%. These results are in agreement with the FE simulations and reflect the fact that the existence of the notch changes the local vibration of the pipe and therefore only affects its adjacent sensor. The second observation is that in some cases these sensors were unable to predict the damage progression (see figure 18 for the unpressurized pipe case). It is believed that the source of this discrepancy refers to the inherent errors involved in experimental vibration analysis, such as noise or inconsistency in manually impacting the pipe by the impulse hammer.

It is worth mentioning that unlike the FE results, the analysis of the signals from the sensors located at the right side of the weld (RPZTs) registered small EMD-EDI amplitudes, with a poor indication of damage and its progression, even for the sensor within the damage vicinity. This disagreement between FE simulations and experiments could be related to the fact that, in the FE model, the weld material was assumed to be the same as the pipe's material, while in reality they would not be the same. According to the guidelines given in DNV-RP-F108 [24], not only the material properties of the weld metal would be different from that of the pipe, but also the pipe's material's property would change in the heat affected zone in comparison to the non-heat affected area in the pipe. Consequently, it appears that the difference in the material properties of the pipe, the heat affected zone of the pipe, and the weld material adversely affects the transfer of local vibration in the pipe from one side of the girth weld to the other side.

The experimental EMD-EDI obtained from the velocity signals acquired by the LDV for the damage cases of the top and side notch are reported in figure 21. This figure includes data for both pressurized and unpressurized conditions. For the case of the bottom notch, no data was recorded by the LDV because of access limitation to the bottom of the pipe with the LDV. As shown in figure 21, for each damage location only the EMD-EDI from adjacent sensors are depicted. These are L1L/L1R and L7L/L7R for the top and side notches, respectively. Refer to figure 15 for the LDV measurement locations on the pipe. Analysis of the results at other locations revealed either small or meaningless amplitudes for the EMD-EDI and, thus, are not reported.

From figure 21 it is clear that for both the unpressurized and pressurized pipes, the EMD-EDI calculated at L1L and L7L, respectively, could identify the existence of the top and side notches. Furthermore, as the damage severity increased the damage index rose accordingly. Surprisingly, for the case of the top notch, a sharp jump can be observed in the damage index calculated at location L1L. Similar to data from the PZT sensors, the EMD-EDI values calculated at the right side of the weld (locations L1R and L7R) were unsatisfactory for notch detection. The amplitude of damage indices at these locations is not noticeable and, moreover, they do not follow the progression of the damage.

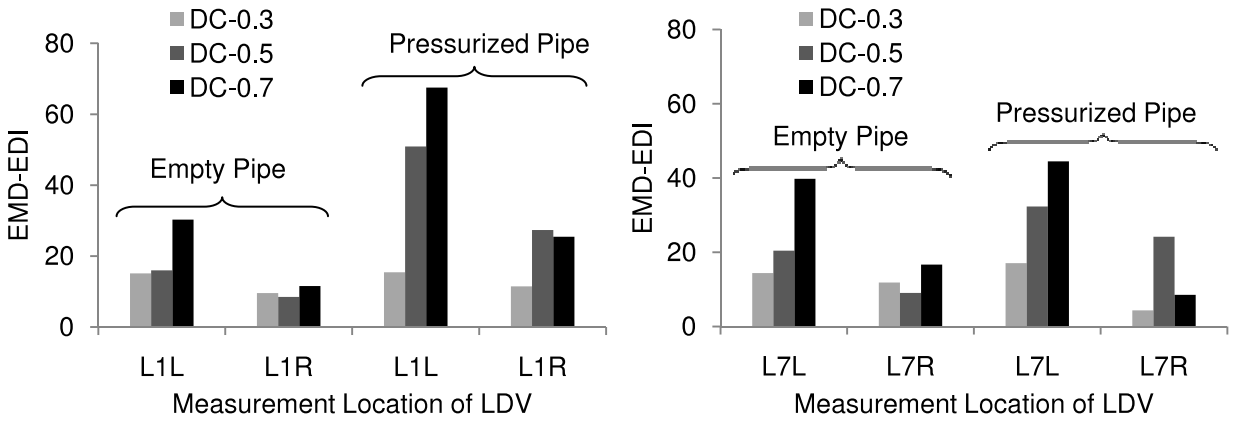

Figure 21. Experimental EMD-EDI evaluated from the first IMF of the LDV for the unpressurized and pressurized pipe: (left) top notch; (right) side notch.

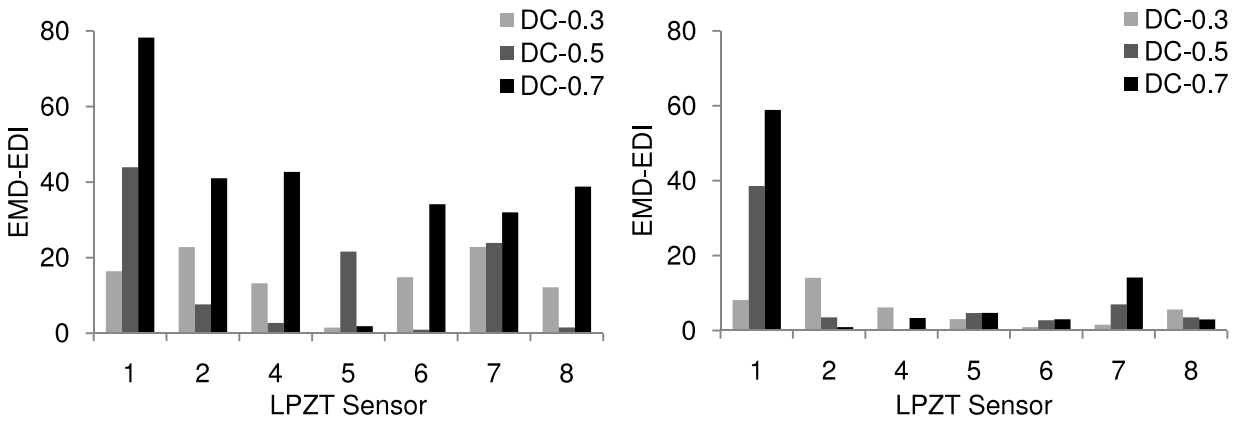

Figure 22. Experimental EMD-EDI evaluated from the second IMF of the PZT sensors for the pipe with a top notch. (Left) Unpressurized pipe; (right) pressurized pipe.

Regardless of the discrepancies mentioned above, figures 18–21 provide sound evidence of the capability of the damage index EMD-EDI in notch detection as well as in notch quantification in the girth weld of pipeline. To emphasize the superiority of this index as opposed to methods based on changes in the natural frequencies, the natural frequencies of the pipe were experimentally extracted from the signals of PZT sensors before creating the notch and also after each damage case. As an example, for the case of pressurized pipe with the top notch DC-0.7 the natural frequencies of LPZT2 were examined over the range of 0–3 KHz. The greatest change in frequencies between the intact and notched pipe was calculated as 0.54% for a frequency of 183.0 Hz. The predicted value of EMD-EDI for the same damage case was 57.3%.

The insensitivity of the longitudinal/circumferential frequencies to the circumferential notch observed above is in agreement with the outcomes of Srinivasan and Kot [10], and also with the fact that orientation of such defects will not break the axial symmetry [11]. This further highlights the advantage of the EMD-EDI method for crack detection in pipeline girth weld.

6.2. Experimental EMD-EDI results based on the second IMF

As mentioned before, the EMD-EDI is based on the variation of the first IMF energy before and after occurrence of damage. In an attempt to refine this concept, and to further investigate the EMD-EDI potential capabilities in damage detection, the same methodology was applied to the second IMF of the PZT signals acquired from the vibration of the unpressurized and pressurized pipe. Typical results of this investigation are presented in figures 22–24 for the top, side, and bottom notch cases, respectively. Similar to the first IMF, it can be seen that LPZT1 for the top notch, LPZT7 for the side notch, and LPZT5 for the bottom notch could provide clear indication of damage existence, as well as its severity. For each case, the other sensors further away from the damage poorly identified the damage, except for the case of unpressurized pipe with the top notch DC-0.7 (for which 6 sensors registered significant damage indices). In general, the second IMF performed almost as sensitively and effectively as the first IMF in notch identification in pipe's girth weld. One can also sum the damage indices obtained from analysis of the first and second IMFs in order to get a higher resolution for damage identification.

6.3. Experimental investigation of the instantaneous phase

After successful implementation of the first and second IMF energies for damage detection through the EMD-EDI methodology, other aspects of the HHT were also examined

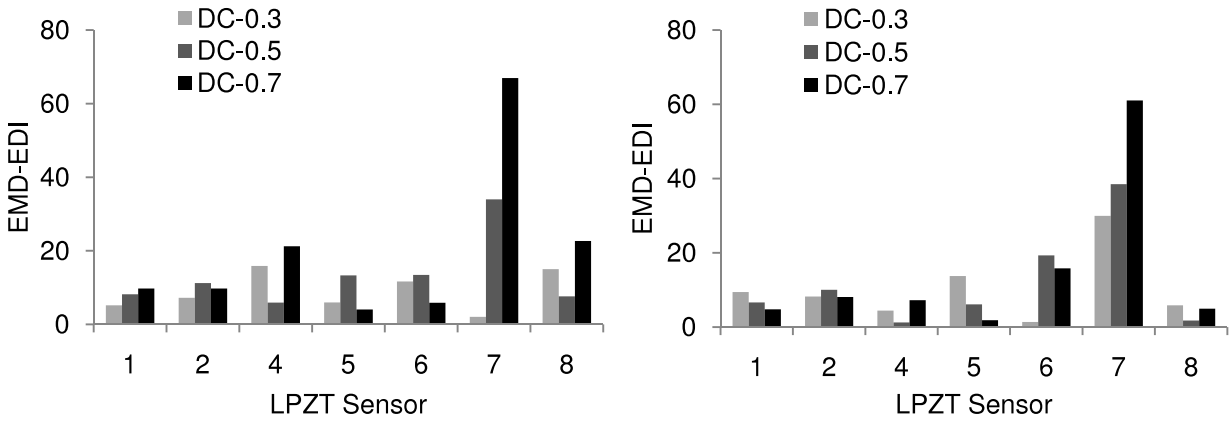

Figure 23. Experimental EMD-EDI evaluated from the second IMF of the PZT sensors for the pipe with a side notch. (Left) Unpressurized pipe; (right) pressurized pipe.

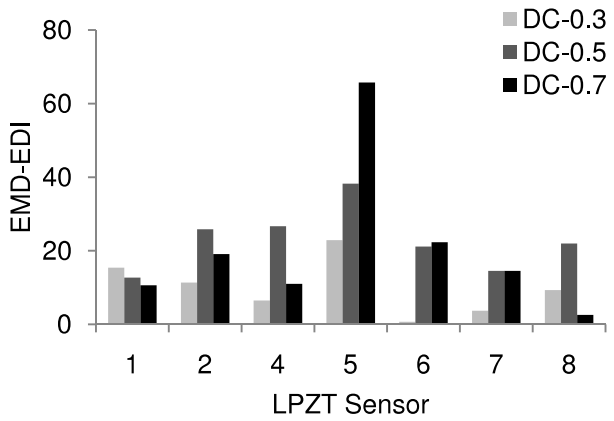

Figure 24. Experimental EMD-EDI evaluated from the second IMF of the PZT sensors for the unpressurized pipe with a bottom notch.

to assess their sensitivity to structural damage. One of these features is the instantaneous phase, which has also been investigated by other researchers, and of which a comprehensive study was published by Pines and Salvino [12]. This work introduced a health monitoring approach, utilizing magnitude, phase, and damping information derived from the HHT to extract the incident energy propagating through the structure. This was implemented through a dereverberation concept, which was based on the change in the speed of propagating waves due to local changes in the properties of the structure induced by damage. A metric was also introduced to identify damage, based on the relative phase of the IMFs between successive degrees of freedom of the system. The proposed method was experimentally validated by determining the damage location and its extent in a three-story civil building model. Damage was created by decreasing the stiffness or mass at specific floors.

In the present study, it was attempted to process the IMFs through equation (3) in order to directly extract and compare the instantaneous phase data of the structure, before and after creating the notch. A preliminary study on the data obtained from the sensors in the notch proximity indicated that the phase data of the first IMF has the greatest sensitivity to the notch. Figure 25 represents typical results of this study for the unpressurized pipe, consisting of the phase data obtained from LPZT1 (i.e., for the top notch), LPZT7 (i.e., for the side notch) and LPZT5 (i.e., for the bottom notch).

It should be noted that after impacting the pipe, the PZT signals lasted at least 2.0 s before decaying to zero. For the instantaneous phase results presented in figure 25, the first 1.0 s of the signals were analyzed instead of the 0.5 s that was used for damage detection based on the first or second IMF. This was done because by increasing the signal length, the phase lag between the undamaged and damaged pipe would be more distinguishable.

From figures 25(a) and (c), it can be observed that in the case of the top and bottom notches, the existence of the notches generated a lag in the instantaneous phase when comparing the data of the healthy and damaged case DC-0.3. This phase lag also increased as the notch depth grow to DC-0.5; however, the difference in data between DC-0.5 and DC-0.7 is indistinguishable. Another observation is that the registered phase lag for the bottom notch is much larger than that for the top notch. This could be a result of pipe sagging, thereby closing the top notch (thus lowering the severity of the damage), while at the same time opening the bottom notch (thus increasing the severity of the damage).

For the case of the side notch (figure 25(b)), the instantaneous phase does not show any change between the healthy and damaged case DC-0.3; however, it registers a noticeable lag for DC-0.5 and more interestingly, the lag increases as the notch depth grows to D-0.7.

From figure 25, it may be concluded that the presence of a notch in the girth weld is reflected by a lag in the instantaneous phase of the signal of the sensor adjacent to the notch. However, this phase lag does not consistently follow the progression of the damage. Although Pines and Salvino [12] found that the phase data produced a good indication of the damage progression, their data were calculated analytically from a 3DOF mass and spring system in which the damage was taken in the form of reduction in the stiffness of one of the springs by 25%, 50%, and 75%, which is considered to be a large decrease in the stiffness values due to damage. It is therefore believed that the inconsistency seen in the phase lag

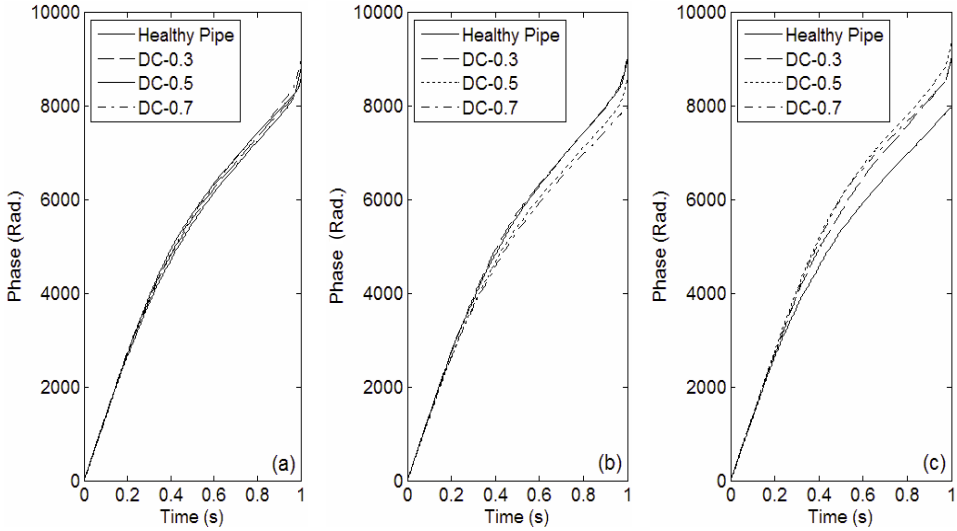

Figure 25. Instantaneous phase calculated by the HHT from the first IMF for different damage cases on the unpressurized pipe. (a) Top notch data from LPZT1; (b) side notch data from LPZT7; (c) bottom notch data from LPZT5.

values in the case of the notches considered in the present study is due to the fact that the notches cause insignificant impact on the stiffness of the system. In summary, this aspect of the work requires more investigation.

Further inspection of figure 25 reveals that, in the presence of damage, the instantaneous phase increases for the top and bottom notches (figures 25(a) and (c)), but decreases for the side notch (figure 25(b)). A reason for this phenomenon could be the fact that the top and bottom notches are in symmetric locations and, therefore, they would experience similar vibration patterns, while the vibration pattern would be slightly different for the side notch.

7. Remarks on the notch and crack

As mentioned before, this study is based on the detection of an artificially induced notch on the girth weld. However, real cracks are often generated due to fatigue loading, and generally behave differently from the notches. The difference between notches and cracks becomes more evident due to crack closure during vibration, especially in cracks located at the compression side of a pipe. As stated by Gounaris [29], a fatigue crack on the compression side remains closed during vibration, and thus would have no effect on the natural frequencies of the pipe. However, in most pipeline cases, the vast majority of cracking occurs at the tension side of the pipes. This occurs in the field, mainly due to the tensile loading resulting from the free spanning of the pipes, both on-shore and off-shore. Moreover, pipelines are normally under internal pressure, which further induces crack opening forces. In addition to these facts, the proposed health monitoring method could detect a notch despite there being no change in the frequencies before and after the presence of the flaw. Thus, it is believed that both proposed approaches in this study (i.e., the EMD-EDI and instantaneous phase methodologies) are capable of detecting cracks in pipeline girth welds.

8. Conclusion

In the present work the application of the EMD and HHT for crack detection in girth welds of a suspended steel pipeline was numerically and experimentally investigated. The basic concept was to analyze the pipe vibration signals through the EMD and HHT, coupled with two different damage sensitive parameters. The first is a damage index, referred to as the EMD-EDI, which was established based on an energy comparison of the first or second IMF of the vibration signals captured before and after occurrence of the damage. The second parameter is an evaluation of the lag in the instantaneous phase derived from the HHT. For crack simulation, a narrow notch was created at one side of the weld. Different notch depths and locations were examined. The pipe's local vibration in the weld vicinity was monitored using two different means: (i) by the use of PZT sensors and (ii) by employing a LDV. To insure the capability of the proposed methods in practical applications, the pipe was tested under both unpressurized and internally pressurized conditions.

Results from both the numerical and experimental investigations showed that, in all damage cases, the EMD-EDI determined based on either the first or second IMF of the PZT sensor, or the LDV's signals in the notch vicinity, could detect the presence of the notch and, more importantly, could follow the progression of the notch size qualitatively. However, other sensors and locations far from the notched area were almost insensitive to the presence of the notch. It was also observed that, for crack detection purposes, band pass filtering of the signals is a crucial step of the process, and that it should be carefully applied such that only the sensitive frequency components to the crack are passed and the others are filtered out. A comparative study of the EMD energy damage index with a method based on changes in the natural frequencies of the pipe revealed the advantage of the proposed damage index in terms of high sensitivity and effectiveness.

Analysis of the instantaneous phase data of the PZT sensors, in proximity to the damage, revealed that the presence of damage in the pipe manifests as a lag in local phase data. Consequently, the instantaneous phase could successfully detect the presence of the notch, but could not predict the progression of damage as effectively.

The present study focused on the detection of notches in girth welds. However, it is believed that the method can be successfully applied for crack detection, since cracks are often found on the tension side of a pipe, thus under the dynamic state they would remain open due to the tensile stresses, much like the dynamic response of a notch.

Overall, the proposed health monitoring technique in this study can be regarded as a relatively simple, low cost, and effective NDT tool, which does not require sophisticated and expensive equipment. The preliminary results from this approach are interpreted as an encouraging step towards establishing a practical and reliable structural health monitoring procedure for pipeline girth welds.

Despite the successful implementation of the HHT and EMD methods on the laboratory scale, some practical issues are involved when considering real applications. For instance, the proposed damage detection methodology requires periodic monitoring of the pipeline using PZT sensors or the use of a LDV. While PZT sensors are low cost and light weight, and capable of producing a high signal to noise ratio with no added mass effects on the structure, nevertheless, their downside is that a large number of them should be bonded adjacent to each girth weld on a given pipeline. On the other hand, the LDV is a portable device with the capability of making accurate velocity measurement, but comparatively, it produces lower resolution in damage identification. Consequently, one way to make the use of PZT sensors economically and practically viable may be developing a system by which the PZT sensors could scan the girth weld area without having to bond them to the pipe. The viability of this idea is being currently explored by our research group.

Acknowledgment

The financial support of the Petroleum Research Atlantic Canada (PRAC) in this work is gratefully acknowledged.

References

[1] Stetson J T 2008 Advancements in pipeline girth weld inspection *17th World Conf. on Nondestructive Testing (Shanghai, China, Oct. 2008)*

[2] Fortunko C M and Schramm R E 1982 Evaluation of pipeline girth welds using low-frequency horizontally polarized waves *J. Nondestruct. Eval.* **3** 155–73

[3] Lumb F R 1977 Inspection of pipelines using nondestructive techniques *J. Phys. Technol.* **8** 249–56

[4] Kim J-T, Ryu Y-S, Cho H-M and Stubbs N 2003 Damage identification in beam-type structures: frequency-based method versus mode-shape-based method *J. Eng. Struct.* **25** 57–67

[5] Shi Z Y, Law S S and Zhang L M 2000 Structural damage detection from modal strain energy change *J. Eng. Mech.* **126** 1216–23

[6] Ren W-X and De Roeck G 2002 Structural damage identification using modal data II: test verification *J. Struct. Eng.* **128** 96–104

[7] Owolabi G M, Swamidas A S J and Seshadri R 2003 Crack detection in beams using changes in frequencies and amplitudes of frequency response functions *J. Sound Vib.* **265** 1–22

[8] Kim J T 2003 Crack detection in beam-type structures using frequency data *J. Sound Vib.* **259** 145–60

[9] Nahvi H and Jabbari M 2005 Crack detection in beams using experimental modal data and finite element model *Int. J. Mech. Sci.* **47** 1477–97

[10] Srinivasan M G and Kot C A 1992 Effect of damage on the modal parameters of a cylindrical shell *10th Int. Conf. on Modal Analysis (San Diego)* pp 529–35

[11] Wake R N and Evans J T 1999 The effect of cracks on the natural frequencies of axi-symmetric vibration modes of gas cylinders *J. Eng. Fract. Mech.* **64** 177–91

[12] Pines D and Salvino L 2006 Structural health monitoring using empirical mode decomposition and the Hilbert phase *J. Sound Vib.* **294** 97–124

[13] Tua P S, Quek S T and Wang Q 2005 Detection of cracks in cylindrical pipes and plates using piezo-actuated Lamb waves *J. Smart Mater. Struct.* **14** 1325–42

[14] Krawczuk M 2002 Application of spectral beam finite element with a notch and iterative search technique for damage detection *J. Finite Elements Anal. Design* **38** 537–48

[15] Quek S T, Wang Q, Zhang L and Ang K K 2001 Sensitivity analysis of notch detection in beams by wavelet technique *Int. J. Mech. Sci.* **43** 2899–910

[16] Huang N E, Shen Z, Long S R, Wu M C, Shih H H, Zheng Q, Yen N C, Tung C C and Liu H H 1998 The empirical mode decomposition and the Hilbert spectrum for nonlinear and non-stationary time series analysis *Proc. R. Soc.* A **454** 903–95

[17] Xu Y L and Chen J 2004 Structural damage detection using empirical mode decomposition: experimental investigation *J. Eng. Mech.* **130** 1279–88

[18] Lin S, Yang J N and Zhou Li 2005 Damage identification of a benchmark building for structural health monitoring *J. Smart Mater. Struct.* **14** 162–9

[19] Cheraghi N, Riley M J and Taheri F 2005 A novel approach for detection of damage in adhesively bonded joints in plastic pipes based on vibration methods using piezoelectric sensors *IEEE SMC Int. Conf. on Systems, Man and Cybernetics (Hawaii, USA, Oct 2005)* vol 4 (Piscataway, NJ: IEEE) pp 3472–8

[20] Cheraghi n and Taheri F 2007 A damage index for structural health monitoring based on the empirical mode decomposition *J. Mech. Mater. Struct.* **2** 43–62

[21] Rezaei D and Taheri F 2009 Experimental validation of a novel structural damage detection method based on empirical mode decomposition *J. Smart Mater. Struct.* **18** 1–14

[22] Rezaei D and Taheri F 2009 A novel application of laser doppler vibrometer in a health monitoring system *J. Mech. Mater. Struct.* at press

[23] 2000 *Specification for Line Pipe, API Specification 5L* 42 edn, January

[24] 2006 Recommendation Practice, DNV-RP-F108 *Fracture Control for Pipeline Installation Methods Introducing Cyclic Plastic Strain* DET NORSKE VERITAS, January

[25] Chati M, Rand R and Mukherjee S 1997 Modal analysis of a cracked beam *J. Sound Vib.* **207** 249–70

[26] GE Oil & Gas 2009 *Pipeline Inspection & Integrity Services/Inspection Services/Crack Detection/Types of cracks/Girth Weld Cracks* accessed http://www.geoilandgas.com/

[27] Fung Y C, Sechler E E and Kaplan A 1957 On the vibration of thin cylindrical shells under internal pressure *J. Aeronaut. Sci.* **24** 650–61

[28] Zhang Y L, Gorman D G and Reese J M 2003 Vibration of prestressed thin cylindrical shells conveying fluid *J. Thin-Walled Struct.* **41** 1103–27

[29] Gounaris G, Anifantis N and Dimarogonas A D 1991 Dynamics of cracked hollow beams *J. Eng. Fract. Mech.* **39** 931–40